effective than DMF in disrupting the peptide aggregates.

DMF, being less effective, is capable of discriminating the stability of the β-structure of the Boc side chain protected Orn homopentapeptide from those of the same pentapeptide with two different sequences of mixed side-chain protection (Boc and Adoc) at high concentration (40 mg/mL) (Figure 3). Clearly, the intentional interruption of the uniformity of the Boc protecting groups in the Orn side chains decreases the stability of the β-structure of the corresponding peptides. Interestingly, Moroder et al. have recently reported that disruption of the uniformity of the *tert*-butyl alcohol derived protecting groups in a synthetic somatostatin fragment, by blocking the ε-amino function of a Lys residue as the Adoc derivative, exerts a strong solubility effect.[4]

Conclusions

We have shown that main-chain length, specific amino acid sequence, concentration, and uniformity of side-chain protection are all factors playing a role on the stability of the peptide self-aggregated species. It is gratifying to note that the (quantitative) scales of increasing tendency of the peptides to self-aggregate in solution, determined in this work, parallel the (qualitative) scales of their decreasing solubility properties.[10,15] Incidentally, the hierarchies of the propensity of the peptides to assume strongly hydrogen bonded structures in the solid state[21] are in full agreement with those found in solution. We have also demonstrated that IR absorption is a useful technique to titrate quantitatively the extent of self-aggregation in peptides. In general, the titration of the 1630-cm^{-1} band can be carried out more accurately than that of the 3290-cm^{-1} band. However, at high DMF percentages the short-frequency tail of the amide band of the solvent overlaps the 1630-cm^{-1} absorption. Concentrations close to those usually employed in peptide synthesis (40–50 mg/mL) and N^{α}-deblocked peptides in the presence/absence of added tertiary amine[8,9] are also suitable for this study. We believe that this method will be of profit to chemists interested in the synthesis of medium-sized peptides, often poorly reactive owing to strong self-association and low solubility.

Acknowledgment. The expert technical assistance of Vittorio Moretto is gratefully acknowledged.

Registry No. Z-[L-Orn(Boc)]$_5$-OMe, 85571-69-3; Z-(L-Val)$_2$-Orn-(Boc)-OMe, 85571-67-1; Z-L-Orn(Boc)-(L-Val)$_2$-L-Orn(Boc)-OMe, 88376-82-3; Z-[L-Orn(Boc)]$_2$-(L-Val)$_2$-L-Orn(Boc)-OMe, 88376-83-4; Z-[L-Orn(Boc)]$_3$-L-Orn(Adoc)-L-Orn(Boc)-OMe, 88376-84-5; Z-L-Orn(Adoc)-[L-Orn(Boc)]$_2$-L-Orn(Adoc)-L-Orn(Boc)OMe, 88391-94-0.

(21) Toniolo, C.; Bonora, G. M., unpublished observations.

Transition-State Structural Features for Anilide Hydrolysis from β-Deuterium Isotope Effects[1a]

Ross L. Stein,[1b] Hisashi Fujihara, Daniel M. Quinn,[1c] G. Fischer, G. Küllertz, A. Barth, and Richard L. Schowen*

Contribution from the Department of Chemistry, University of Kansas, Lawrence, Kansas 66045, and the Department of Biochemistry, Biosciences Section, Martin Luther University, DDR-4020 Halle, German Democratic Republic. *Received August 8, 1983. Revised Manuscript Received October 14, 1983*

Abstract: The hydrolysis in basic aqueous solution of p-$NO_2C_6H_4NHCOCH_3$ and p-$NO_2C_6H_4NHCOCD_3$ at 30 °C from $[HO^-]$ = 0.002 to 2.31 M generates observed isotope effects k_o^H/k_o^D that begin in the least basic solution at 0.967 ± 0.011, pass through a maximum of around 0.98 at $[HO^-]$ about 0.03 M, and then fall to 0.933 ± 0.020 in the most basic solution. This phenomenon arises from a base-dependent mixture of rate-limiting transition states. At the lowest base concentrations, decomposition of the uninegative tetrahedral adduct, with k_2^H/k_2^D = 0.94 ± 0.02, dominates. In the intermediate range, decomposition of the dinegative adduct, with k_3^H/k_3^D = 1.00 ± 0.02, becomes important. In the most basic solutions, nucleophilic attack of hydroxide on the substrate (k_1^H/k_1^D = 0.94 ± 0.01) assumes the major role. These isotope effects are consistent with quasi-tetrahedral transition states for formation and decomposition of the uninegative adduct and with rate-limiting trapping or diffusional separation of $\{CH_3CO_2^-, ArNH^-\}$ for decomposition of the dinegative adduct. The observed isotope effect at $[HO^-]$ = 0.208 M seems to show an anomalously large dependence on temperature, changing from 0.944 ± 0.016 at 3.8 °C to 0.977 ± 0.019 at 50 °C, which generates on an Arrhenius model A_H/A_D = 1.17 and ΔE_a = 117 cal mol^{-1}. The data are shown, however, also to be fully consistent with a different model: a shift in limitation of the rate away from the k_1 transition state toward the k_3 transition state, as the temperature is raised, and with simple zero-point-energy origins for the individual isotope effects.

Secondary hydrogen isotope effects can be used to deduce the structural features of transition states,[2-5] and the technique is being used for this purpose in the investigation of enzyme catalytic power.[3-5] However, in many complex reaction systems, including both enzymic and nonenzymic examples, a number of different processes may simultaneously contribute to limiting the reaction rate. Then the observed isotope effect may be a complicated average of the effects on the elementary steps.[6,7] Alternatively

Scheme I

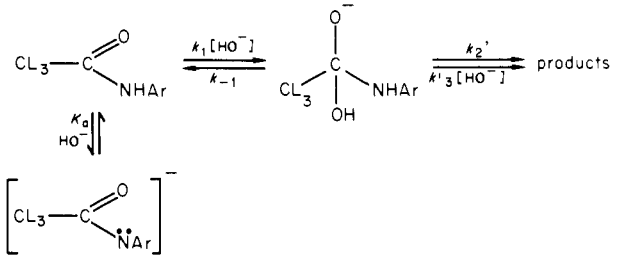

(1) (a) Research in Lawrence was supported through Grant GM-20198 by the National Institute of General Medical Sciences. (b) Current address: Pulmonary Pharmacology, ICI Americas Inc., Wilmington, DE 19897. (c) Current address: Department of Chemistry, University of Iowa, Iowa City, IA 52242.

(2) Shiner, V. J., Jr. In "Isotope Effects in Chemical Reactions", Collins, C. J., Bowman, N. S., Eds.; Van Nostrand-Reinhold: Princeton, NJ 1970; Chapter 2.

(3) Kirsch, J. F. In "Isotope Effects on Enzyme-Catalyzed Reactions"; Cleland, W. W., O'Leary, M. H., Northrop, D. B., Eds.; University Park Press: Baltimore, 1977; pp 100–121.

(4) Hogg, J. L. In "Transition States of Biochemical Processes"; Gandour, R. D., Schowen, R. L., Eds.; Plenum Press: New York, 1978; Chapter 5.

(5) Cleland, W. W. *Method. Enzymol.* **1982**, *87C*, 625.

0002-7863/84/1506-1457$01.50/0

Table I. Rate Constants[a] for the Basic Hydrolysis of p-$NO_2C_6H_4NHCOCL_3$ (L = H, D) in Aqueous Solution[b]

$10^2 \times$ [HO⁻], M	$10^6 k_o \pm$ SD, s^{-1}		
	L = H	L = D	$k_o^H/k_o^D \pm$ SD
231	9889 ± 95	10598 ± 198	0.933 ± 0.020
100	4110 ± 49	4359 ± 20	0.943 ± 0.013
20.8	617 ± 4	637 ± 4	0.973 ± 0.009
7.53	128.6 ± 1.5	132.9 ± 0.8	0.968 ± 0.013
2.80	26.90 ± 0.14	27.49 ± 0.26	0.979 ± 0.011
1.00	4.178 ± 0.024	4.261 ± 0.016	0.981 ± 0.007
0.50	1.355 ± 0.012	1.407 ± 0.007	0.964 ± 0.010
0.30	0.710 ± 0.011	0.732 ± 0.006	0.969 ± 0.010
0.20	0.471 ± 0.007	0.487 ± 0.007	0.967 ± 0.011

[a] Corrected for substrate ionization according to eq 1. [b] At 30.17 ± 0.05 °C, μ 0.50 with KCl.

stated, the isotope effect arises from the properties of a number of transition states (and sometimes reactant states). The "intrinsic" effects for the individual processes are the most valuable ones, since they relate the properties of a single transition state to the properties of a single reactant state. Their extraction from the observed effects is thus desirable, but it is often difficult. This is particularly true when, as is frequently the case, the kinetic law is complicated. In principle, the intrinsic effects may be extracted by direct fitting of data for two isotopic reactants independently to the rate law to obtain values of the component rate constants. Such an approach requires many values of the observed rates or rate constants, all of very high precision.

This situation is exemplified in the hydrolysis of anilides in basic solution[8-10] (Scheme I, L = H, D), which serves as a model for the action of various important enzyme classes, particularly amidases and proteases. This reaction is dauntingly slow in rate so that precise rate constants cannot readily be measured. Further, the observed rate constants k_{obsd} must first be corrected for substrate ionization (eq 1) and then fitted to the formidable

$$k_o = k_{obsd}[(K_w + K_a[HO^-])/K_w] \quad (1)$$

expression of eq 2, where $k_2 = k_2'(k_1/k_{-1})$, and $k_3 = k_3'(k_1/k_{-1})$.

$$k_o = \{k_1[HO^-](k_2 + k_3[HO^-])/(k_1 + k_2 + k_3[HO^-])\} \quad (2)$$

Attempts to obtain the rate constants from eq 2 by nonlinear least-squares analysis may fail from "ill conditioning".[11]

A great improvement for such cases has been introduced by Stein,[7] who advocates treating observed isotope effects (velocity ratios or ratios of k_{obsd} under corresponding conditions) as appropriate weighted averages of the intrinsic isotope effects. By the use of his approach, isotope effects for individual processes may be isolated without high-precision, complete kinetic analysis of both isotopic reactions. Here we apply this technique to obtain the β-deuterium isotope effects for the component processes in Scheme I, finding that the results are different in part from those previously arrived at by more conventional methods.[10]

Results

Observed Isotope Effects vs. Hydroxide Concentration. Table I shows rate constants k_o at various hydroxide concentrations for the hydrolysis of p-$NO_2C_6H_4NHCOCL_3$ (L = H, D) at 30 °C in water. These rate constants refer to the unionized anilide as effective initial state since they have been corrected according to eq 1; the values pK_a(L = H) = 13.73, pK_a(L = D) = 13.72, determined by titration, were employed. Also given in the table are the ratios k_o^H/k_o^D, the observed isotope effects.

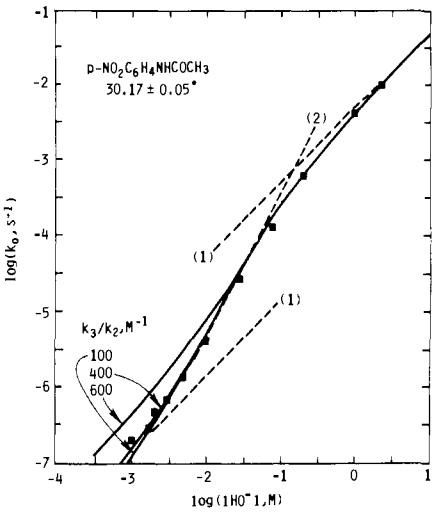

Figure 1. Doubly logarithmic plot of k_o (corrected for substrate ionization) vs. [HO⁻] for hydrolysis of p-$NO_2C_6H_4NHCOCH_3$ at 30.2 °C. The lines drawn through the data correspond to eq 2, with 10^3k_1 = 4.47 M^{-1} s^{-1}, 10^2k_3 = 4.7 M^{-2} s^{-1}, and k_2 defined by the ratios indicated. The dashed lines show slopes of one or two.

The rate constants k_o^H are plotted logarithmically vs. log [HO⁻] in Figure 1. Nonlinear least-squares fitting of the data to eq 2 gives $k_1 = (4.47 \pm 0.01) \times 10^{-3}$ M^{-1} s^{-1} and $k_3 = (4.7 \pm 0.2) \times 10^{-2}$ M^{-2} s^{-1} but k_2 is not well-defined. Curves are shown in Figure 1 for k_3/k_2 = 100, 400, and 600 M^{-1}. Values in the range of 100–400 seem to be favored. Similar results are obtained with k_o^D.

In this situation, it is clear that the isotope effects could be calculated from the least-squares parameters reasonably well for k_1 (which is determined to ±0.2%), much less well for k_3 (which is determined to ±4%), and not at all for k_2. Therefore the method of Stein was used.

According to this approach, the observed isotope effect is taken as a weighted average of the isotope effects for the individual processes. The rate constants k_1, k_2, and k_3 all have the free reactants, hydroxide ion, and p-$NO_2C_6H_4NHCOCL_3$ as effective reactant states, so that their relative weights reflect the contributions of their respective transition states to the virtual transition state[6,7] under any set of conditions. The forms of the weighting function and weighting factors can be derived as follows. Inverting eq 2, we write eq 3 for the deuterated substrate. Multiplying by

$$(k_o^D)^{-1} = (k_1^D[HO^-])^{-1} + ([HO^-]\{k_2^D + k_3^D[HO^-]\})^{-1} \quad (3)$$

k_o^H, we obtain eq 4 for the observed isotope effect. The final term

$$(k_o^H/k_o^D) = (k_o^H/(k_1^H[HO^-]))(k_1^H/k_1^D) + k_o^H([HO^-]\{k_2^D + k_3^D[HO^-]\})^{-1} \quad (4)$$

of eq 4 can be further manipulated as in eq 5. Finally we have

$$k_o^H/([HO^-]\{k_2^D + k_3^D[HO^-]\}) = 1/([HO^-]\{(k_2^D/k_2^H) \times (k_2^H/k_o^H) + (k_3^D/k_3^H)(k_3^H[HO^-]/k_o^H)\}) \quad (5)$$

eq 6 with C_1, C_2, and C_3 defined by eq 7. A different weighting

$$(k_o^H/k_o^D) = C_1(k_1^H/k_1^D) + ([C_2(k_2^H/k_2^D)]^{-1} + [C_3(k_3^H/k_3^D)]^{-1})^{-1} \quad (6)$$

$$C_1 = k_o^H/(k_1^H[HO^-]) \quad (7a)$$

$$C_2 = k_o^H/(k_2^H[HO^-]) \quad (7b)$$

$$C_3 = k_o^H/(k_3^H[HO^-]^2) \quad (7c)$$

function which is valid for small isotope effects on k_2 and k_3 was derived and used by Stein.[7] Note that the weighting factors depend solely on data for the *protiated* substrate.

(6) Schowen, R. L. In "Transition States of Biochemical Processes"; Gandour, R. D., Schowen, R. L., Eds.; Plenum Press: New York, 1978; Chapter 2.
(7) Stein, R. L. *J. Org. Chem.* **1981**, *46*, 3328.
(8) Pollack, R. M.; Bender, M. L. *J. Am. Chem. Soc.* **1970**, *92*, 7190. Pollack, R. M. *J. Org. Chem.* **1974**, *39*, 2108.
(9) DeWolfe, R. H.; Newcomb, R. C. *J. Org. Chem.* **1971**, *36*, 3870.
(10) Küllertz, G.; Fischer, G.; Barth, A. *Tetrahedron* **1976**, *32*, 759.
(11) Kershner, L. D.; Schowen, R. L. *J. Am. Chem. Soc.* **1971**, *94*, 2014.

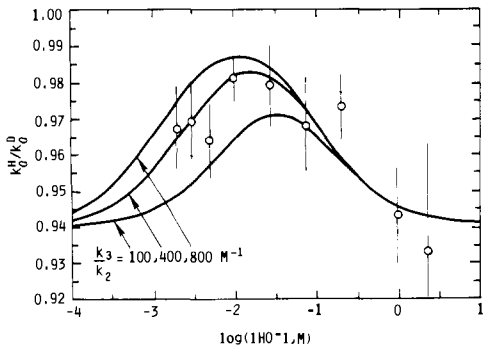

Figure 2. Plot of observed isotope effect (k_o^H/k_o^D) vs. log [HO$^-$] for hydrolysis of *p*-$No_2C_6H_4NHCOCL_3$ (L = H, D) at 30.2 °C. The three lines correspond to eq 6 and 7 with 10^2k_1 = 4.47 M^{-1} s^{-1}, 10^2k_3 = 4.7 M^{-2} s^{-1}, and k_2 defined by the ratios indicated. For all three curves, the mean isotope effects (k_1^H/k_1^D = 0.94; k_2^H/k_2^D = 0.94; k_3^H/k_3^D = 1.00) were employed.

The data of Table I were fitted to eq 6 by a nonlinear least-squares method with k_1 and k_3 as above and with k_2 given various values. The resulting isotope effects (with standard deviations) are as follows:

10^4k_2, M^{-1} s^{-1}	k_1^H/k_1^D (SD)	k_2^H/k_2^D (SD)	k_3^H/k_3^D (SD)
4.70	0.936 (0.005)	0.959 (0.006)	1.015 (0.011)
1.20	0.940 (0.006)	0.944 (0.010)	0.996 (0.008)
0.60	0.941 (0.006)	0.932 (0.015)	0.991 (0.008)

We conclude therefore that the isotope effects lie in the ranges k_1^H/k_1^D = 0.94 ± 0.01; k_2^H/k_2^D = 0.94 ± 0.02; k_3^H/k_3^D = 1.00 ± 0.02. The observed isotope effects are plotted against log [HO$^-$] in Figure 2, and three calculated curves, corresponding to the three choices of k_2 shown above, are drawn in.

Stein's approach thus allows us to obtain values of three isotope effects, to precisions of 1–2%, in a system where only one of the absolute rate constants can be determined with good precision (k_1, determined to about 0.2%), a second is known only to 4% precision, and the third is known at best only within a factor of 10. In fact, considering the data in this paper alone, the isotope-effect plot of Figure 2 is the best evidence that the k_2 process exists. The absolute rate data in Figure 1 could be fitted reasonably well setting k_2 = 0 and allowing appropriate adjustment of k_1 and k_3 (not done in the lines shown in Figure 1). Figure 2, in contrast, demands that three different rate processes contribute since threee distinct isotope-effect regions are visible: $k_o^H/k_o^D \sim 0.96$–0.97 at [HO$^-$] = 10^{-3}–10^{-2} M (dominance of k_2 process); $k_o^H/k_o^D \sim 0.98$ at [HO$^-$] = 10^{-2}–10^{-1} M (incursion of the k_3 process); $k_o^H/k_o^D \sim 0.93$ at [HO$^-$] > 1 M (dominance of the k_1 process). If only two rate processes were present, then Figure 2 would have the form of a simple titration curve.

Observed Isotope Effects vs. Temperature. Table II presents values of k_{obsd}^H and k_{obsd}^D at a single hydroxide ion concentration of 0.208 M, at temperatures from 3.8 to 50 °C. The isotope effects of k_{obsd} at each temperature are also given. If, as expected, the lack of isotope effect on K_a, observed at 30 °C, holds at all temperatures, then these are also the isotope effects k_o^H/k_o^D.

Discussion

The extraction of reasonably precise isotope effects for each of the kinetic terms in this complex reaction system shows the power of the Stein approach. Notable features[7] of the approach are that:

(a) Rate constants for only one isotopic form are required to construct the weighting factors.

(b) The resulting isotope effects are very insensitive to the exact values of the rate constants used in the weighting factors. Thus a rough kinetic analysis for one isotopic compound, combined with a careful set of observed isotope effects, leads to good definition of the intrinsic isotope effects for the individual kinetic terms.

Reaction Progress at the Transition States. The β-deuterium isotope effects on the individual rate processes can be related to the structures of the corresponding transition states. As previously,[12] we take the quantity $\hat{I}$ defined by eq 8 to measure the

Table II. Temperature Dependence of Observed Rate Constants and Isotope Effects for Hydrolysis of *p*-$NO_2C_6H_4NHCOCL_3$ (L = H, D) in Aqueous Solution[a]

temperature, °C	10^6k_{obsd} ± SD, s^{-1}		k_{obsd}^H/k_{obsd}^D ± SD
	L = H	L = D	
3.8 ± 0.1	40.1 ± 0.1	42.5 ± 0.7	0.944 ± 0.016
5.0 ± 0.1	45.4 ± 0.3	47.9 ± 0.5	0.954 ± 0.012
15.00 ± 0.05	111.9 ± 1.2	117.8 ± 0.2	0.950 ± 0.010
25.00 ± 0.05	269.9 ± 1.4	280.3 ± 1.7	0.963 ± 0.008
30.00 ± 0.05	405.7 ± 2.9	418.9 ± 2.6	0.969 ± 0.009
40.00 ± 0.05	864 ± 5	898 ± 9	0.962 ± 0.011
50.00 ± 0.1	1815 ± 22	1857 ± 28	0.977 ± 0.019

[a] [HO$^-$] = 0.208 M, μ 0.50 with KCl.

$$k_H/k_D = (K_H/K_D)^{\hat{I}} \quad (8)$$

degree to which the transition-state acyl function has altered its structure from trigonal ($\hat{I}$ = 0) toward tetrahedral ($\hat{I}$ = 1). The limiting effect K_H/K_D is assumed to be 0.87 ± 0.04 for CH_3 vs. CD_3, obtained from the equilibrium isotope effect for ketone hydration,[12] with the generous error limits meant to allow for possible steric or electronic contributions specific to particular systems. The results are as follows:

$$CH_3CONHAr + HO^- \xrightarrow{k_1} TS1^- \qquad \hat{I} = 0.44 \pm 0.16$$

$$CH_3CONHAr + HO^- \xrightarrow{k_2} TS2^- \qquad \hat{I} = 0.44 \pm 0.21$$

$$CH_3CONHAr + 2HO^- \xrightarrow{k_3} TS3^{2-} \qquad \hat{I} = 0.00 \pm 0.21$$

The k_1 process, corresponding most likely to attack of hydroxide on the substrate carbonyl function, yields an $\hat{I}$ suggesting substantial tetrahedral character, perhaps around 50%, at the transition state. Attack of hydroxide on phenyl esters, as distinct from this anilide, shows[12] $\hat{I} \sim 0.2$–0.4. This rather small value may arise from the probable significance[12-15] of desolvation of the nucleophile prior to bond formation. With reactive electrophiles like esters, the desolvated hydroxide ion may react with a quite early transition state and small $\hat{I}$. *p*-Nitroacetanilide is, however, 400 times less reactive than phenyl acetate toward hydroxide ion. Thus a later transition state, and larger $\hat{I}$, are reasonable.

The k_2 process probably has a transition state that corresponds to expulsion of the leaving group $ArNH^-$ from the uninegative tetrahedral intermediate, most likely with some protolytic assistance from solvent (conceivably leading directly to $ArNH_2$). At least, such assistance is indicated by solvent isotope effects in the hydrolysis[11] and methanolysis[16] of trifluoroacetanilides, although the extension to unactivated acetanilides is admittedly speculative. If such assistance is present, the k_2 transition state is that for protolytically assisted leaving-group expulsion. In the reverse of the k_2 reaction, this would be protolytically assisted attack of nitroaniline on the carboxyl group. The transition-state structure must, of course, be the same in both directions. Several examples of the protolytically assisted nucleophilic attack of water at ester carbonyl show[12] $\hat{I}$ = 0.58–0.65. The value obtained here, 0.44 ± 0.21, is near this range.

Perhaps the most surprising result is for the k_3 transition state: $\hat{I}$ = 0.00, corresponding to an essentially trigonal structure for the transition-state carbonyl group. This transition state is

(12) Kovach, I. M.; Elrod, J. P.; Schowen, R. L. *J. Am. Chem. Soc.* **1980**, *102*, 7530.
(13) Hupe, D. J.; Jencks, W. P. *J. Am. Chem. Soc.* **1977**, *99*, 451.
(14) Kovach, I. M.; Hogg, J. L.; Raben, T.; Halbert, K.; Rodgers, J.; Schowen, R. L. *J. Am. Chem. Soc.* **1980**, *102*, 1991.
(15) Jencks, W. P.; Brant, S. R.; Gandler, J. R.; Fendrich, G.; Nakamura, C. *J. Am. Chem. Soc.* **1982**, *104*, 7045.
(16) Hopper, C. R.; Schowen, R. L.; Venkatasubban, K. S.; Jayaraman, H. *J. Am. Chem. Soc.* **1973**, *95*, 3280.

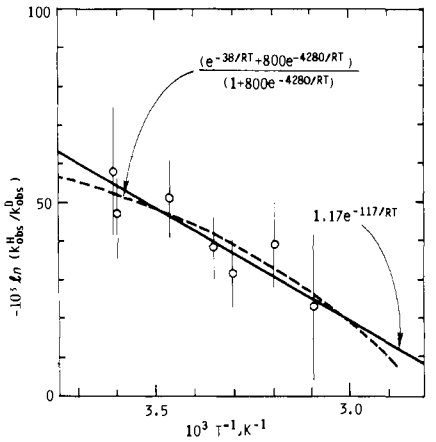

Figure 3. Temperature dependence of k_o^H/k_o^D for hydrolysis of *p*-$NO_2C_6H_4NHCOCL_3$ (L = H, D) at $[HO^-] = 0.208$ M. The straight, solid line is a fit to the Arrhenius function $(k_H/k_D) = (A_H/A_D)\exp(-E_a/(RT))$ with the result shown. The curved, dashed line is a fit to eq 13 with the best fit parameters indicated.

probably for overall leaving-group expulsion from the dinegative tetrahedral intermediate, possibly with some involvement of proton donation to the departing nitrogen.[11,15] One hypothesis that is consistent with the value of $\hat{I} = 0.00$ is shown in eq 9 If one or

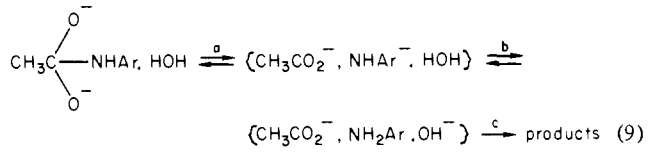

(9)

both of the steps labeled b or c should determine the rate, the carbonyl structure would be trigonal in the transition state. These steps correspond to trapping of the anionic leaving group by solvent (or general acid when present) or to diffusion of the product species apart. The trigonal carbonyl structure in either case would lead to $\hat{I} = 0.00$.

Comparison with Previous Work. The present method of determination of the isotope effects gives, in the case of k_1^H/k_1^D, an effect in approximate agreement with the previous estimate of Küllertz, Fischer, and Barth[10] (0.94 ± 0.01 vs. the earlier value of 0.90 ± 0.03). For k_3^H/k_3^D, both old and new values are the same: 1.00 ± 0.02 here; 1.00 ± 0.03 earlier. In the case of k_2^H/k_2^D, the present method gives 0.94 ± 0.02 while the earlier value was 1.08 ± 0.03. It is not surprising that this effect is not well determined by standard methods. In the concentration range $[HO^-] \simeq 10^{-3}$–10^{-2} M, where earlier k_o^H/k_o^H was taken as approximately equal to k_2^H/k_2^D, our weighting factors give C_1 = 0.04–0.12, C_2 = 0.68–0.18, and C_3 = 0.28–0.70. Thus while C_2 does to some degree dominate in part of this region, this dominance amounts to no more than 70%.

Temperature Dependence. The temperature dependence of the isotope effect, as portrayed in Figure 3, is also much better understood by use of weighting factors. Although the error limits overlap throughout the temperature range, the mean isotope effects define a suggestive trend toward unity as the temperature rises. This is expected but the degree of change is not. Thus the solid straight line drawn through the data in Figure 3 corresponds to eq 10. This is the typical Arrhenius-ratio treatment of isotope-effect temperature dependences,[17] which generates a preexponential factor A_H/A_D and a difference in isotopic activation energies ΔE_a. The preexponential factor A_H/A_D of 1.17 is far larger than expected (it should be unity[17]), and the apparent activation-energy difference ΔE_a is so great that much more inverse isotope effects would have been generated if it were not for the large A_H/A_D. At 25 °C, for example, the observed isotope effect of 0.96 would have been represented as a product (1.17)(0.82). Neither of these factors has a good physical rationale.

$$k_{obsd}^H/k_{obsd}^D = 1.17e^{-117/(RT)} \quad (10)$$

An alternative and simpler fit to the data is provided by the curved, dashed line in Figure 3. This is generated by the following procedure. First were note that at 30 °C and 0.208 M hydroxide ion, $C_1 = 0.69$, $C_3 = 0.31$, and $C_2 \sim 0$. Then eq 6 becomes

$$k_o^H/k_o^D = C_1(k_1^H/k_1^D) + C_3(k_3^H/k_3^D) \quad (11)$$

We assume the simplest possible zero-point-energy temperature dependences for k_1^H/k_1^D (=0.94 at 30 °C) and k_3^H/k_3^D (=1.00 at 30 °C):

$$k_1^H/k_1^D = e^{-38/(RT)} \quad (12a)$$

$$k_1^H/k_1^D = 1.00 \quad (12b)$$

Inserting these into eq 11, recalling that $C_1 = 1 - C_3$ and that $C_1 = 1/(1 + [k_1/(k_3[HO^-])])$, we have

$$k_o^H/k_o^D = [e^{-38/(RT)} + \alpha e^{-\beta/(RT)}]/[1 + \alpha e^{-\beta/(RT)}] \quad (13)$$

where

$$R \ln \alpha = \Delta S_1^\ddagger - \Delta S_3^\ddagger - R \ln [HO^-] \quad (14a)$$

$$\beta = \Delta H_1^\ddagger - \Delta H_3^\ddagger \quad (14b)$$

The curved line in Figure 3 is drawn for $\alpha = 800$ (thus $\Delta S_1^\ddagger - \Delta S_3^\ddagger = 10$ cal K^{-1} mol^{-1}) and $\beta = 4280$ cal mol^{-1}; obtained by nonlinear least-squares fitting of the isotope effects to eq 13. As is readily seen,the fit is not worse than that for the Arrhenius-ratio treatment. Furthermore, the result is consistent with simple zero-point-energy origins for the intrinsic isotope effects, which leads to no sensible variation in the intrinsic effects over this temperature range ($k_1^H/k_1^D = e^{-38/(RT)} = 0.932$ at 0 °C and 0.942 at 50 °C). The apparent variation in k_{obsd}^H/k_{obsd}^D arises on this model from a temperature-induced shift in rate-determining step. At 0 °C, $C_1 = 0.78$, $C_3 = 0.22$, $k_{obsd}^H/k_{obsd}^D = (0.78)(0.932) + (0.22)(1.00) = 0.947$. At 50 °C, $C_1 = 0.50$, $C_3 = 0.50$, $k_{obsd}^H/k_{obsd}^D = (0.50)(0.942) + (0.50)(1.00) = 0.971$. This shift is produced by a perfectly reasonable difference in transition-state enthalpies of 4.3 kcal mol^{-1} and in transition-state entropies of 10 cal K^{-1} mol^{-1}, between the transition states for the k_1 and k_3 processes (of the protiated substrate).

Conclusions. The Stein approach[7] leads to readily interpreted values of the β-deuterium secondary isotope effects for each of the kinetic terms in *p*-nitroacetanilide basic hydrolysis and to a simple understanding of the temperature dependence of the overall effect in strongly basic solution. The corresponding transition-state structures are the expected quasi-tetrahedral ones for formation and breakdown of the uninegative adduct of anilide and hydroxide ion. Breakdown of the dinegative adduct may occur with protolytic trapping or a diffusional process as rate determining.

Experimental Section

Materials and Solutions. *p*-$NO_2C_6H_4NHCOCH_3$ (PNAA) and *p*-$No_2C_6H_3NHCOCD_3$ (PNAA-d_3) were prepared by the reaction of *p*-nitroaniline with CH_3COCl or CD_3COCl (Merck; 99% deuterated) in either pyridine at room temperature or benzene containing dimethylaniline at 10 °C or in dry ether with pyridine at 0 °C. The anilides were each 3 times recrystallized from MeOH, yielding yellow crystals melting at 214 °C (lit.[10] mp 215–216 °C). With some samples, reprecipitation from acetone/*n*-hexane gave mp 214.5 °C, purity by GC >99%. Deuterium incorporation was estimated by NMR to be no less than 95% and by GC–MS to exceed 98%. Aqueous sodium hydroxide solutions were either dilutions of a Fisher certified standard 1.000 N solution or prepared from sodium hydroxide pellets (Mallinckrodt Analytical Reagent). These solutions were then allowed to stand at 5 °C for several hours to precipitate carbonates, filtered by gravity, and degassed with N_2 before being sealed in plastic bottles. Hydroxide concentrations were determined the day of kinetic experiments by titration of potassium hydrogen phthalate to a phenolphthalein end point. Water used to prepare solutions was distilled from a copper-bottom still, passed through a Barnsted mixed-bed ion-exchange column, and finally distilled from glass. Acetonitrile used for the preparation of substrate stock solutions was Fisher Certified A.C.S. grade.

(17) Melander, L.; Saunders, W. H., Jr. "Reaction Rates of Isotopic Molecules"; Wiley: New York, 1980; pp 73–75.

Determination of pK_a Values for PNAA and PNAA-d_3. The pK_a values of PNAA and PNAA-d_3 were determined spectrophotometrically at 410 nm by using hydroxide concentrations of 2.0×10^{-2} to 2.0 M (μ = 1.0 M with NaCl, except for [OH^-] > 1 M). The dissociation constants were calculated from plots of OD/[PNAA-l_3] vs. 1/[OH^-] according to Hine and Hine.[18] The pK_a's are 13.73 for PNAA and 13.72 for PNAA-d_3 agreeing with previous values for PNAA of 13.6 and 13.8. The isotope effect on the equilibrium constant is $K_a^H/K_a^D = 0.98 \pm 0.04$ and agrees with the previous value[10] of 0.998 (no error limits reported).

Kinetics. Rates of *p*-nitroaniline production were measured spectrophotometrically at 410 nm with automatic data acquisition, with a Cary 16-Hewlett-Packard minicomputer system.[19] Reactions were initiated by the injection of small aliquot (10-50 μL) of a stock solution of the anilide in acetonitrile into a cuvette, usually of 1-cm path length, containing 3.00 mL of hydroxide solution. Reaction temperatures were controlled by a Lauda K4/RD circulating bath connected to the cuvette holder. Temperatures were monitored by a thermistor device with digital readout. For hydroxide concentrations of 0.208 M and greater, rates were determined under first-order conditions. First-order rate constants were obtained by weighted nonlinear least-squares analysis, commonly of 1000 data points. Zero-under conditions were employed for hydroxide concentrations less than 0.208 M. Reaction mixtures containing 1 mM substrate were monitored at 410 nm for 10-60 min, corresponding to less than 0.5% reaction in all cases (absorbance change 0.01-0.05). First-order rate constants were calculated according to

$$k_{obsd} = (dA/dt)/[\text{PNAA-}l_3]\Delta\epsilon_{410}$$

Substrate concentrations were based on gravimetric determinations, after demonstrating spectrophotometrically that the materials were sufficiently pure to allow this. $\Delta\epsilon_{410}$ is the extinction coefficient difference between *p*-nitroacetanilide and *p*-nitroaniline (PNA). This value is independent of isotopic substitution but is dependent on [HO^-] since PNAA, which does not absorb at 410 nm, ionizes to produce a chromophoric anion ($PNAA^-$). Thus

$$\Delta\epsilon_{410} = \epsilon_{PNA} - (\epsilon_{PNAA^-})[K_a/(K_a + [H^+])]$$

where ϵ_{PNA} at 410 nm is 9.20×10^3 M^{-1} cm^{-1}, and ϵ_{PNAA^-} at 410 nm is 4.63×10^3 M^{-1} cm^{-1}. In all studies, rates for protiated and deuterated substrates were measured in alternation.

For runs at very low [HO^-], a special buretting setup was used, which kept the solution under N_2 while it was introduced into a 5-cm cell. Reaction was initiated by injection through a serum cap of 500 μL of stock substrate solution in acetonitrile into 13 mL of base solution. Again, the two isotopic substrates were studied in alternation.

Registry No. *p*-$NO_2C_6H_4NHCOCH_3$, 104-04-1; *p*-$NO_2C_6H_4NHCOCD_3$, 88548-58-7; CH_3COCl, 75-36-5; CD_3COCl, 19259-90-6; *p*-nitroaniline, 100-01-6; deuterium, 7782-39-0.

(18) Hine, J.; Hine, M. *J. Am. Chem. Soc.* **1952**, *74*, 5266.
(19) Hegazi, M. F.; Borchardt, R. T.; Schowen, R. L. *J. Am. Chem. Soc.* **1979**, *101*, 4351.

Enzymes in Organic Synthesis. 31.[1] Preparations of Enantiomerically Pure Bicyclic [3.2.1] and [3.3.1] Chiral Lactones via Stereospecific Horse Liver Alcohol Dehydrogenase Catalyzed Oxidations of Meso Diols

Alexander J. Bridges, P. Sundara Raman, George S. Y. Ng, and J. Bryan Jones*

Contribution from the University of Toronto, Department of Chemistry, Toronto, Ontario, Canada M5S 1A1. *Received August 17, 1983*

Abstract: Preparative-scale horse liver alcohol dehydrogenase catalyzed oxidations of *meso*-1,3-bis(hydroxymethyl)cyclopentyl and -cyclohexyl substrates proceed stereospecifically to give 42-81% yields of the corresponding chiral bridged-bicyclic γ-lactones of 100% ee. For each diol, oxidation of the hydroxymethyl group attached to the *S* center occurs exclusively. The stereospecificites observed are as predicted by the active-site model of the enzyme.

Numerous examples of the broad spectrum of asymmetric synthetic opportunities provided by the use of enzymes as practical chiral catalysts have now been documented.[2] Of particular value in this regard are the abilities of enzymes to induce stereospecific transformations of symmetrical substrates. Meso compounds are one symmetrical-substrate group for which asymmetric enzyme-catalyzed conversions to a range of synthetically useful enantiomerically pure chiral products have been documented.[2] Such reactions require enzymes to discriminate between enantiotopic groups attached to centers of opposite chiralities within the meso substrates. An enzyme that possesses this capability to a synthetically viable degree is horse liver alcohol dehydrogense (HLADH[3]). HLADH is a commercially available NAD-dependent alcohol dehydrogenase that catalyzes CH(OH) $\rightleftharpoons$ C=O oxidoreductions of a wide range of organic chemically significant structures.[1,4,5] In preparative-scale reactions it has been shown to operate stereospecifically on enantiotopic carbonyl groups of meso diones in its reductive mode[5a,b] and to discriminate enantiotopic hydroxyl groups of meso diol substrates under oxidation conditions.[4c,5c] Recently we reported on the ability of HLADH to effect enantiotopically specific oxidations of monocyclic meso *cis*-1,2-diols to chiral lactones.[4c] We have now established that the enzyme remains stereospecific for monocyclic cis-1,3-sub-

(1) Part 30: Jones, J. B.; Takemura, T. *Can. J. Chem.*, in press.
(2) (a) Suckling, C. J.; Suckling, K. E. *Chem. Soc. Rev.* **1974**, *3*, 387. (b) Jones, J. B. In "Enzymic and Nonenzymic Catalysis"; Dunnill, P., Wiseman, A., Blakeborough, N., Eds.; Ellis Horwood/Wiley: Chichester/New York, 1980; pp 54-83; In "Asymmetric Synthesis"; Morrison, J. D., Ed.; Academic Press: New York; Vol. 3 in press. (c) Wong, C.-H.; Whitesides, G. M. *Aldrichimica Acta* **1983**, *16*, 27.
(3) Abbreviations used: HLADH, horse liver alcohol dehydrogenase; NAD, nicotinamide adenine dinucleotide, oxidized form; FMN, flavin mononucleotide (riboflavin phosphate); $Eu(tfc)_3$, tris[((trifluoromethyl)-hydroxymethylene)-(-)-camphorato]europium(III) (optishift I).
(4) (a) Prelog, V. *Pure Appl. Chem.* **1964**, *9*, 119. (b) Graves, J. M. H.; Clark, A.; Ringold, H. J. *Biochemistry* **1965**, *4*, 2655. (c) Ng, G. S. Y.; Yuan, L.-C.; Jakovac, I. J.; Jones, J. B. *Tetrahedron*, in press and previous papers. Jones, J. B.; Beck, J. F. *Tech. Chem. (N.Y.)* **1976**, *10*, 107. (d) Nakazaki, M.; Chikamatsu, H.; Naemura, K.; Suzuki, T.; Iwasaki, M.; Sasaki, Y.; Fujii, T. *J. Org. Chem.* **1981**, *46*, 2726 and previous papers. (e) van Osselaer, T. A.; Lemiere, G. L.; Merckx, E. M.; LePoivre, J. A.; Alderweireldt, F. C. *Bull. Soc. Chim. Belg.* **1978**, *87*, 799. (f) Abril, O.; Whitesides, G. M. *J. am. Chem. Soc.* **1982**, *104*, 1552. (g) MacInnes, I.; NonLebel, D. C.; Orszulik, S. T.; Suckling, C. J., *J. Chem. Soc., Chem. Commun.* **1982**, 121.
(5) (a) Dodds, D. R.; Jones, J. B. *J. Chem. Soc., Chem. Commun.* **1982**, 1080. (b) Nakazaki, M.; Chikamatsu, H.; Taniguchi, M. *Chem. Lett.* **1982**, 1762. (c) Jakovac, I. J.; Goodbrand, H. B.; Lok, K. P.; Jones, J. B. *J. Am. Chem. Soc.* **1982**, *104*, 4659.

0002-7863/84/1506-1461$01.50/0